

## THEORETICAL STUDY OF THE NON-STEADY DISCHARGE AT ATMOSPHERIC PRESSURE IN PIN - PLATE SYSTEM AND ITS APPLICATION FOR OZONE PRODUCTION

*V.I. Karas<sup>1</sup>, V.I. Golota<sup>1</sup>, V.P. Mal'khanov<sup>2</sup>, I.F. Potapenko<sup>3</sup>, O.N. Shulika<sup>1</sup>*

<sup>1</sup>*National Science Center "Kharkov Institute of Physics & Technology", Kharkov, Ukraine, karas@kipt.kharkov.ua, fax: 38(0572)353564*

<sup>2</sup>*TurboDEn, Moscow, Russia, turboden@mail.ru, fax: 7(095)4680332*

<sup>3</sup>*Keldysh Institute of Applied Mathematics of the RAS, Moscow, Russia, irina@KELDYSH.ru, fax: 7(095)9720737*

In this paper as a result of the theoretical studies and a numerical simulation we presented the following main conclusions: (i) for humid air at increasing pressure of  $1.0133 \cdot 10^5$  Pa until  $5.0665 \cdot 10^5$  Pa ozone concentrations during  $2 \cdot 10^{-3}$ s become higher in 22 times. This fact we clear with structure of ozone-production reactions. In this case the harmful  $NO_x$  concentrations are 2-3 order lower than ozone one; (ii) it is shown that nitrogen is useful to ozone production in the discharge; (iii) based on ion collection we cleared increasing ignition discharge voltage at growing ozone concentrations even with low ozone concentrations.

### INTRODUCTION

Electrodynamic and plasma-chemical processes at high-pressure glow discharge conditions have a very complicated, many-factor character, because in the discharge gap there occur nearly simultaneously a great many separate streamer discharges, which cross the discharge space parallel to each other. Generally, one can expect that the discharge characteristics are determined by the energy put into the gas flow. However, it is evident that the resulting gradients of the discharge parameters along the gas flow are not too great, because the specific power density is not high. Therefore the variations in the gas/discharge parameters from one local streamer discharge to another can be neglected. By contrast, the nonuniformity in the discharge parameters in the direction from one electrode to the other should be expected to be very strong. Really, the radius of current channel near the needle is several orders of magnitude smaller than the period of needle separation along the gas flow. This means that the gradients of both the electric field strength and the charged particle density are great, particularly in the vicinity of the needle electrode. So, the two-dimensional model for the glow discharge can be constructed by taking one PCR structure element and formulating the equations, which describe the propagation of the discharge from the needle electrode to the plane electrode.

In atmospheric-pressure air, the nonlocality effects of electron/ion distributions, and also, of diffusion, can play a certain role only at a very small distance from the electrode (cathode dark space). Bearing in mind the insensibility of the parameter of the cathode layer to the choice of the kinetic model, we have chosen the simplest model, where all the transport coefficients and the kinetic coefficients are the local-importance functions of the reduced electric field  $E/N$  ( $E$  is the electric field strength,  $N$  is the gas particle density).

The basic parameters of any electrical discharge in gas are mainly determined by the energy distribution of electrons. The knowledge of electron kinetics of the low

-temperature plasma is of great importance for simulation of plasma-chemical processes in the glow discharge in air. For example, the average energy or the temperature of electrons governs the rate of plasma-chemical processes and the discharge power distribution between different channels. A more exact analysis can be performed with the use of the electron energy distribution function (EEDF), but the experimental determination of the EEDF in plasma is a rather complicated problem. Therefore, various methods of theoretical simulation are in considerable use. A typical theoretical approach to determination of the EEDF in a gas plasma is the solution of the Boltzmann equation in the two-body approximation. This approach appears rather simple and reliable; it is confirmed by comparison with more substantiated methods of simulation, e.g., the Monte-Carlo method.

The electron motion in gas under the action of the external electric field  $E$  is determined by the frequency of collision with molecules and other charged particles. The electron-electron collisions become to play a certain role at a relatively high degree of gas ionization, generally, starting from  $10^{-4}$  -  $10^{-3}$ . Typical electron densities in the discharge are substantially less than  $10^{15} \text{ cm}^{-3}$ , therefore the electron-electron interaction can be neglected to a high accuracy.

The discharge in the gas flow is simulated in the framework of the zero-dimensional model that considers the time evolution of charged particle motion as an evolution of gas portion that is moving together with the gas flow crosswise to the discharge gap. In this model, air is considered as a  $N_2 : O_2 : H_2O$  mixture being in the electrical field which is calculated by solving the equation for the electric circuit involving the electromotive force source, ballast resistance and discharge. In consequence of a rather small energy contribution to the gas, the variations in the gas composition and vibration temperatures can be neglected. The electron-electron, electron-ion collisions and any other collisions of II-type can also be neglected. In this case, all kinetic coef-

ficients for the processes involving electrons are the functions of the reduced electric field  $E/N$  and the gas composition.

### MATHEMATICAL SIMULATION OF KINETIC PROCESSES AT GLOW DISCHARGE CONDITIONS

The mathematical model of discharge, developed here in accordance with [2], makes it possible to calculate the evolution of many important plasma components: ions ( $N_2^+$ ,  $O_2^+$ ,  $O_4^+$ ,  $O^-$ ,  $O_2^-$ ,  $O_3^-$ ), electron-excited particles ( $N_2(A^3\Sigma_u^+)$ ,  $N_2^s, O_2(a^1\Delta)$ ,  $O_2(b^1\Sigma)$ ,  $O(^1D)$ ), atoms ( $N$ ,  $O$ ), ozone ( $O_3$ ), nitrogen oxides ( $NO$ ,  $N_2O$ ,  $NO_2$ ,  $NO_3$ ,  $N_2O_5$ ) and electrons. Here  $N_2^s$  denotes the electron-excited molecule of nitrogen at any level, except for  $A^3\Sigma_u^+$ . In humid air, electrons attach to molecules to form negative ions. The negative ions of most importance are  $O^-$ ,  $O_2^-$ ,  $O_3^-$ ,  $O_4^-$ ,  $H^-$ ,  $OH^-$ ,  $NO_2^-$ ,  $NO_3^-$ ,  $O_2^-(H_2O)$ ,  $O_2^-(H_2O)_2$ ,  $OH^-(H_2O)$  and  $OH^-(H_2O)_2$ .

The electron detachment from negative ions is of great importance, because it influences the plasma conductivity. At a measured average electric field strength of  $\sim 10^4$  V/cm in the discharge gap, the attachment rate is appreciably higher than the electron-impact ionization rate. The other process that leads to electron losses is the electron-ion recombination. The only process that can, in principle, compensate the electron losses is the electron detachment from negative ions. The processes of electron detachment include a simple electron detachment, the associated detachment and photodetachment. For the atmospheric plasma, the last process can be neglected.

It is well known that the addition of water vapor to any weakly ionized gas or plasma exerts a considerable effect on the content of positive and negative ions, and the cluster water ions become the predominant ions. This changes the properties of a weakly ionized environment, because (i) the process of electron detachment from negative cluster ions proceeds very slowly, (ii) the process of dissociative recombination of electrons with positive cluster ions of water goes much quicker than with simple positive ions. The both effects lead to a decrease in the electron density, and hence, in the degree of ionization. Therefore, it is of importance to know the rate constants for cluster water ion formation and breakdown.

In simulation, the processes of  $H_2O$  molecule ionization and dissociative attachment, being of greatest importance for the plasma balance, were characterized by the rate constants in the form of functions of the reduced electric field, which were calculated through the solution of the Boltzmann equation for electrons. At a critical reduced electric field value  $(E/N)_c = 12.4 \cdot 10^{-16}$  V cm<sup>2</sup>, the processes of ionization and attachment equalize each other. This value is often called the equilibrium point. In the absence of detachment processes in the collisions, the equilibrium value of the reduced elec-

tric field must be no less than  $(E/N)_c$ . The detachment processes provide an additional amount of electrons as if from an external ionization source, that gives the possibility to maintain the discharge burning at an electric field lower than the equilibrium value.

The continuity equations for electrons and basic positive and negative ions are solved with the 1D - model, that can be briefly described as follows.

The geometry of discharge is symmetrical with respect to the discharge axis. This means that the continuity equation can be solved in terms of the variables  $(x, r)$ , where  $x$  is the distance from the cathode along the discharge axis,  $r$  is the radius. However, the solution of the two-dimensional nonstationary problem in the physics of discharge is still a serious challenge to computer potentialities. On the other hand, the presentation and treatment of calculations also presents difficulties. The present paper deals with a quasi-one-dimensional numerical model. To derive the equations of this model, we make an assumption that all physical parameters ( $E$ ,  $n_e$ ,  $n_p$ ,  $n_n$ ) are constants in each cross section for the discharge current. This approximation was used, for example, by R. Morrow [1], who assumed the discharge channel to have the cylindrical shape. However, from a great many experiments it is well known that the discharge current is concentrated as a small spot on the needle and occupies a comparatively large area on a flat cathode. If the radius of the current channel is introduced, then it strongly increases from the rod to the plane. The ratio of current channel radii on the negative and positive electrodes makes about  $10^3$ . In agree to A. Napartovich et al [2] we consider the radius of the current channel to be the function of the axial coordinate  $x$ . The problem of choosing the channel shape will be discussed separately. Then, integrating the equation with respect to the cylinder of radius  $r$  and height  $dx$  and taking into account the mentioned constancy of the physical parameters, one can obtain the following equations:

$$\frac{\partial n_e}{\partial t} + \frac{1}{S} \frac{\partial}{\partial x} (S n_e w_e) = (v_i - v_a) n_e + v_d n_n, \quad (1)$$

$$\frac{\partial n_p}{\partial t} - \frac{1}{S} \frac{\partial}{\partial x} (S n_p w_p) = v_i n_e, \quad (2)$$

$$\frac{\partial n_n}{\partial t} + \frac{1}{S} \frac{\partial}{\partial x} (S n_n w_n) = v_a n_e - v_d n_n, \quad (3)$$

$$\frac{1}{S} \frac{\partial}{\partial x} (S E) = - (n_p - n_e - n_n) \frac{e}{\epsilon_0}, \quad (4)$$

where  $S(x)$  is the cross-sectional area of the current channel, which is considered to be the known function of the coordinate  $x$ . The introduction of this function is the key point of this model.

Let us discuss this approximation in greater detail. In reality, the charged particle concentrations and the electric field strength vary in space, both along and across the discharge axis. The assumption that these parameters are the step functions of the radius and turn into zero on the channel surface seems quite natural. Howev-

er, it can be substantiated only with a slow variation of  $S(x)$ , i.e., at  $d(\ln S)/d(\ln x) > 1$ . We ignore this problem assuming the channel shape close to the expected one. The other assumption made in the construction of equations (1) - (4) is that the current channel retains its shape all the time. However, this is of no importance for the corona at steady-state conditions.

Equations (1) - (4) should be supplemented by boundary conditions. The boundary conditions for positive and negative ions are obvious: their concentrations equal zero at the anode and at the cathode, respectively. For electrons, in contrast to R. Morrow [1], we consider only the secondary electron emission caused by the ions. Really, some particular processes in air that would yield an essential amount of secondary photoelectrons are unknown. Therefore, it appears reasonable to neglect them at all. Then the boundary condition for electrons is formulated through the introduction of the secondary ion emission coefficient  $\gamma$ :

$$j_e(0, t) = \gamma j_p(0, t), \quad (5)$$

where  $j_e = n_e w_e$ ,  $j_p = n_p w_p$ . The boundary conditions for the electric field strength were determined directly from eqs. (1) - (4) at each time step. The procedure and a detailed description of the numerical algorithm for the solution of the set of eqs. (1)-(4) can be found in ref. [2].

The solution of the above-described set of equations is a complicated task because of a great difference between the characteristic times of the physical processes, and because of the fact that the parameters to be calculated (electric field, charged particle density) strongly vary in the space between the electrodes. For the numerical solution we use the implicit numerical scheme. The space grid is nonuniform, having a smaller step in the vicinity of the electrodes (in particular, close to the needle tip). The integration step in time  $\tau$  is limited by three conditions:

$$\tau < \min(\Delta / (\mu_e E)), \quad (6)$$

$$\tau < \min(1/v_i, 1/v_a), \quad (7)$$

$$\tau < \tau_M, \quad (8)$$

where  $\Delta$  is the local grid size in space,  $\tau_M = 1/(4\pi\sigma)$  is the Maxwellian time,  $\sigma$  is the plasma conductivity.

To avoid the numerical instability, we put the time dependence of the supply voltage in the following form:

$$U_{suppl} = U_0(1 - 0,9 \exp(-t/\tau_{suppl})), \quad (9)$$

where  $\tau_{suppl} = 20\mu s$  can be considered as a characteristic time of the establishment of steady-state conditions. If it is compared with the time intervals, for which the calculations are made, it can be seen that except for the very beginning, the calculations are performed with a practically stable supply voltage, as is also the case in experiment.

Typically, the total number of numerical grid nodes was 160. The real time integration step ranged between  $10^{-12} - 10^{-11}$ s.

The calculations of concentrations of basic charged components are performed by the above-described one-

dimensional model, where the equations were averaged in the approximation of the given discharge shape, i.e., relying on some experimental data or some other physical concepts we assign the shape of the current channel, over which the continuity equations are averaged. In this case, it is also assumed that all the parameters do not vary in the discharge cross section, but are dependent only on the longitudinal coordinate. The Poisson equation, as opposed to other approaches, is solved in the two-dimensional space (in parabolic coordinates) with the help of integration of the algebraic sum of charged component concentrations using the known Green function [6]  $G = R^{-1}$ :

$$G = 2 \sum_{m=0}^{\infty} \int_0^{\infty} \{ J_m(k\lambda) J_m(k\lambda_0) I_m(k\mu) K_m(k\mu_0) \} k dk \times \\ \times \chi_m \cos[m(\varphi - \varphi_0)], \quad \mu_0 > \mu, \quad (10)$$

where  $\lambda, \mu$  are the paraboloid characteristics,  $J_m$  is the first-order Bessel function,  $I_m, K_m$  are the modified Bessel functions of the imaginary argument.

The resulting from this integration spatial distribution of the potential determines the distribution of the reduced electric field  $E/N$ . The knowledge of this distribution permits the use of a locally zero-dimensional model of chemical kinetics, which takes into account about 100 chemical reactions, owing to the local dependence of the rate constants of the main processes (ionization, attachment, detachment, associative recombination, dissociative recombination, etc.), this being due to the presence of the small parameter  $b = l/\lambda_e$  (where  $l$  is the characteristic electrode size and separation,  $\lambda_e$  is the free path length of the electron between the successive collisions) on account of a high pressure of the gas mixture. The quantitative and qualitative compositions of plasma components, between which collisions occur, are substantially dependent on the degree of nonequilibrium of the system, i.e., on the appreciable excess of the average electron energy over the energies of ions, neutral molecules and atoms. Not to overload the problem, we do not take into account the nonequilibrium in the vibrational level distribution. This can be done at a not too high specific power of the discharge, i.e., for the ozonizers with a high gas flow rate as in our case.

The distribution of gas-mixture chemical components, found at the previous stage, makes it possible to find the space distribution of the electron distribution function and, in accordance with the above-described procedure, to find the space distribution of the ionization, detachment, attachment, etc. coefficients which enter into the set of continuity equations for the main charged components. At our experimental conditions, we can restrict ourselves to the equations for electrons, negative ozone ions ( $O_3^-$ ) and positive oxygen ions ( $O_2^+$ ), the concentrations of which considerably exceed the concentrations of other ions. In our case of rather low concentrations of water vapor (no more than 1%), the  $OH^-$  concentration, as indicated by the calculations of the local chemical kinetics, does not approach  $O_3^-$ , and therefore, we calculate only three mentioned kinds

of charged particles. Note that the electron concentration is often several orders of magnitude lower than the ion concentrations, yet, owing to a high mobility of electrons and large cross sections for the processes involving electrons, the equation for electrons is major in the set.

## Results and discussions

The numerical simulation results give the characteristic spatial distribution of the electric field strength and charged particle concentration profiles as functions of the distance from the needle-type electrode at different voltages applied to the discharge gap. Among reactive particles, of most interest for our consideration is ozone which is produced in the discharge as a result of oxygen molecule dissociation. It is well known that for the destruction of ozone produced in the discharge two catalytic cycles are of importance: one is associated with nitrogen oxides, and the other - with hydrogen radicals.

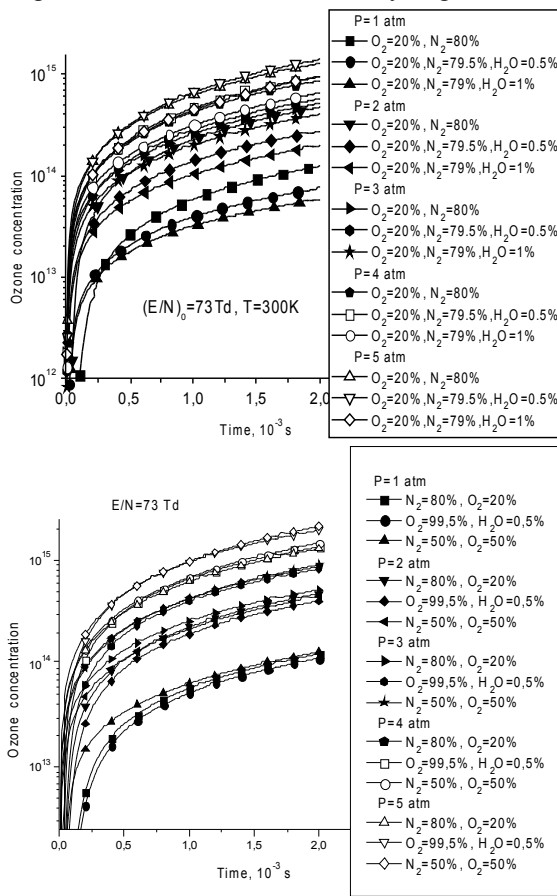


Fig. 1. Ozone concentrations for gas mixtures of various compositions at different pressures

The first cycle can play a significant role only at a great energy contribution that was not attained in the calculations. The other can be the cause of the ozone destruction also at a rather great energy contribution and a high content of water vapor.

The introduction of a small quantity of water vapor may cause the ozone concentration to increase, because, first of all, the discharge voltage increases at the same current value. At a higher voltage, the rate of oxygen molecule dissociation is higher, and this fact plays a positive role for the efficiency of ozone generation. The real ozone yield is the result of competition between

two effects: (i) voltage increase and (ii) the ozone breakdown in the corresponding catalytic cycle. As it is obvious, for our conditions the other aspect of the water vapor effect (that leads to a decreased ozone concentration) becomes of greater importance at  $H_2O$  concentration higher than 1%.

Below (see Fig.1) we give the time evolution of the ozone concentration for various gas mixtures (dry and humid air, combined mixtures) at different parameters (pressure, initial reduced electric field values). The temperature was chosen to be 300 K. For air with a 1% water content, as the pressure rises from 1 atm. to 5 atm., the ozone concentration increases 22 times (see Fig. 1) at a reduced electric field strength  $E/N \approx 73$  Td (1 Td =  $10^{-17}$  V/cm<sup>2</sup>), i.e., an approximately square pressure dependence of ozone concentration takes place, that can be explained on the basis of the structure of basic reactions, where ozone is synthesized.

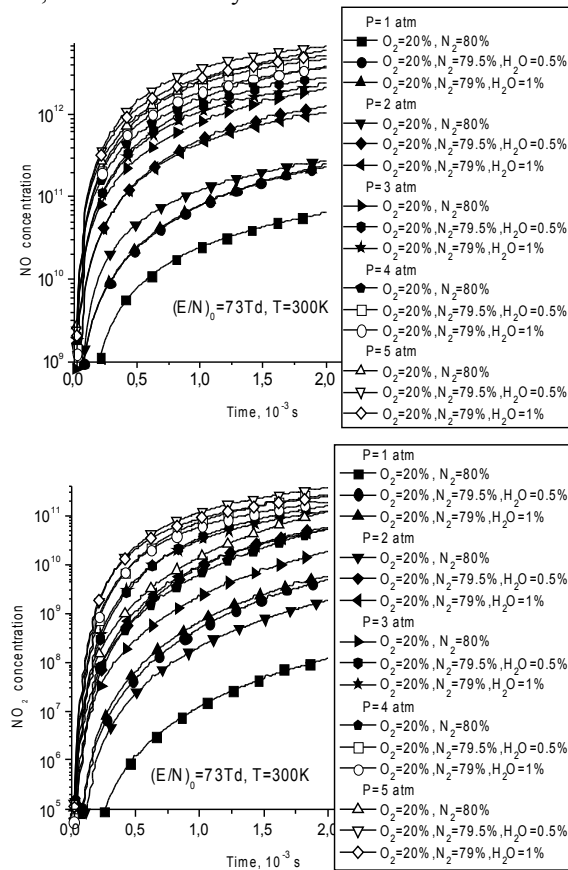


Fig. 2. NO and NO<sub>2</sub> concentrations for dry and humid air at different pressures

In this case, the concentration of harmful  $NO_x$  compounds (see Fig. 2) is 2-3 orders of magnitude lower than the ozone concentration. Therefore, no excess of boundary-admissible concentrations of  $NO_x$  can be provided at rather high ozone concentrations. For the gas mixture  $O_2 : H_2O = 99,5 : 0,5$  at a 5-fold rise in pressure, the ozone concentration increases by a factor of 15 at a voltage even slightly higher than the reduced electric field. The temperature dependence of the ozone concentration (see Fig. 3) obviously shows that this concentration increases with temperature lowering (corresponding increase of neutral particle density in the gas mixture). However, it should be noted that in this case

the specific efficiency remains nearly constant, i.e., the use of cooling may appear expedient to create ozonizers with a higher ozone concentration. We note that here we did not take into account the consumption of energy for cooling, that might be a significant part of the total power expended.

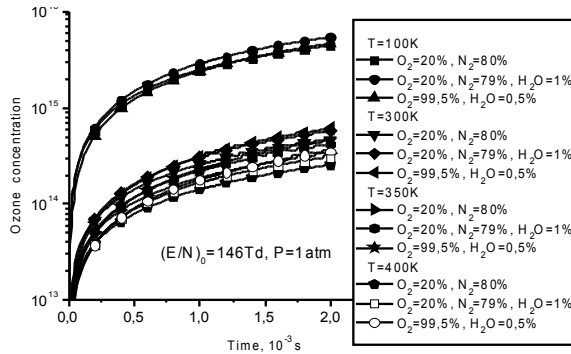


Fig. 3. Ozone concentration for various gas mixtures at different temperatures

For dry air, with a five-fold rise in pressure the electron concentration increases 35 times (from  $2 \cdot 10^6$  to  $7 \cdot 10^7 \text{ cm}^{-3}$ ), see Fig. 4. And at the same rise in pressure for the mixture  $O_2 : H_2O = 99,5 : 0,5$  the increase in the electron concentration does not exceed a factor of 6 (see Fig. 4). As to the gas mixture  $N_2 : O_2 = 50 : 50$ , here the increase in the electron concentration does not exceed a factor of 3 at a five-fold rise in pressure. The comparison of the obtained numerical results shows the following trends: (i) the higher is the humidity, the lower is the discharge current at the same voltage, or a higher voltage is required to maintain the same current value; (ii) the total quantity of nitrogen oxides decreases with a successive replacement of the basic sort of oxide, i.e.,  $N_2O$  by  $NO$ ; (iii) the variations in the concentrations and composition of hydrogen-containing particles are comparatively small. At a higher humidity, the discharge in air approaches the thermodynamically equilibrium discharge. At 2% of  $H_2O$  and higher, it is  $OH^-$  that becomes the main negative ion. It is of interest to note that for 1% and 2% of  $H_2O$ , the evolution of electron concentrations is not monotone. Among the particles produced in the discharge, the  $OH^-$  radicals are the most reactive. It can be seen that their concentration first increases, then reaches maximum and decreases. However, the duration of the increase strongly depends on the water vapor content. This behavior results in a complicated dependence of the maximum  $OH^-$  radical concentrations on time and the water vapor content.

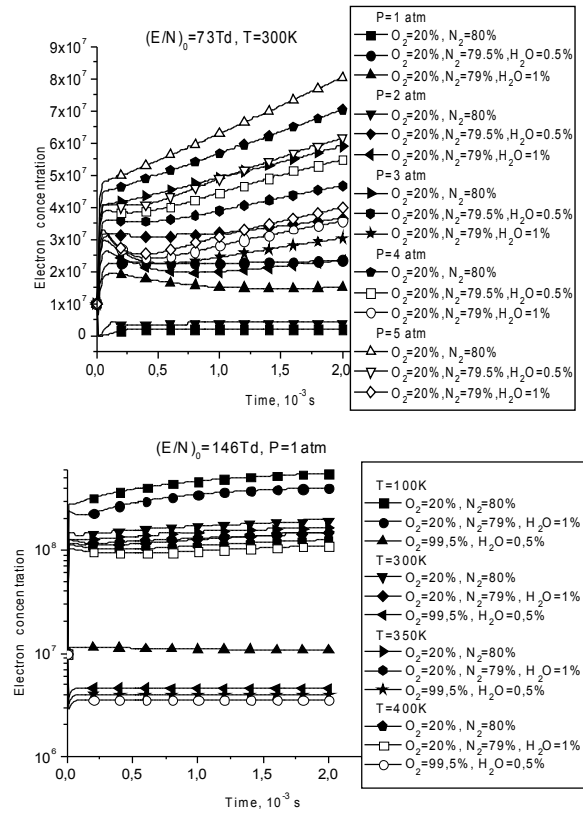


Fig. 4. Electron concentration for dry and humid air at different pressures and temperatures

The electron energy dependence of the electron distribution function is a very illustrative characteristic of the discharge (see Fig. 5).

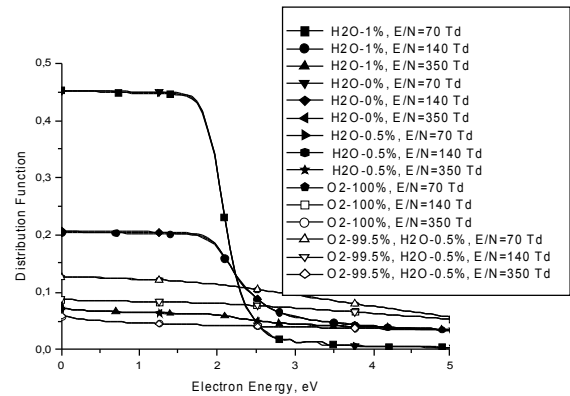


Fig. 5. Electron energy distribution functions for various gas mixtures at different values of the initial reduced electric field  $E/N$

Thus, it can be seen that the distribution function reaches the energy up to 5 - 6 eV with an increase in the reduced electric field from  $E/N \approx 62 \text{ Td}$  up to 350 Td. However, in this case, the behavior of the distribution function very strongly depends on the gas mixture composition. In particular, for the  $O_2 : H_2O = 99,5 : 0,5$  mixture the distribution function is nearly constant in a wide energy range (up to 10 eV). This indicates that there is no effective channel of energy loss by electrons almost up to 10 eV.

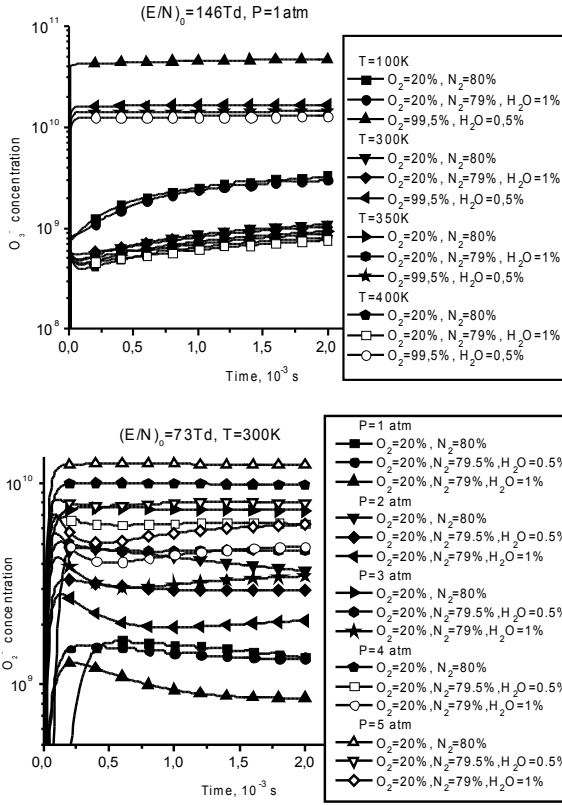


Fig. 6. Concentration of negative ions  $O_3^-$  for various gas mixtures at different temperatures and pressures

The phenomenon known but not explained in the literature, namely, the rise in the discharge ignition voltage with an increasing ozone concentration, can be rather well accounted for relying on two facts: (i) the ion current is 20 to 40 times higher than the electron current, and (ii) as a result of a great cross section for attachment, the  $O_3^-$  ions are the basic ions, their concentration is more than 3 orders of magnitude higher than the concentration of electrons. Therefore, despite the fact that the ozone concentration makes about a few tenths of percent of the oxygen molecule concentration, the both gases are electronegative; a high concentration of  $O_3^-$  ions (they are just responsible for the basic current transfer in the discharge) exerts a cardinal effect on the current-voltage characteristic of the discharge, specifically, on the ignition voltage.

The role of negative  $OH^-$  ions is very significant even at a low water content in the gas mixture (see Fig.7). These ions assist the decrease of electrons in the discharge, take up a substantial portion of ion current and lead to the formation of complex cluster ions.

To compare on Fig. 8 it is shown the concentrations of  $OH$  neutrals in various gas mixtures (humid) at different pressures.

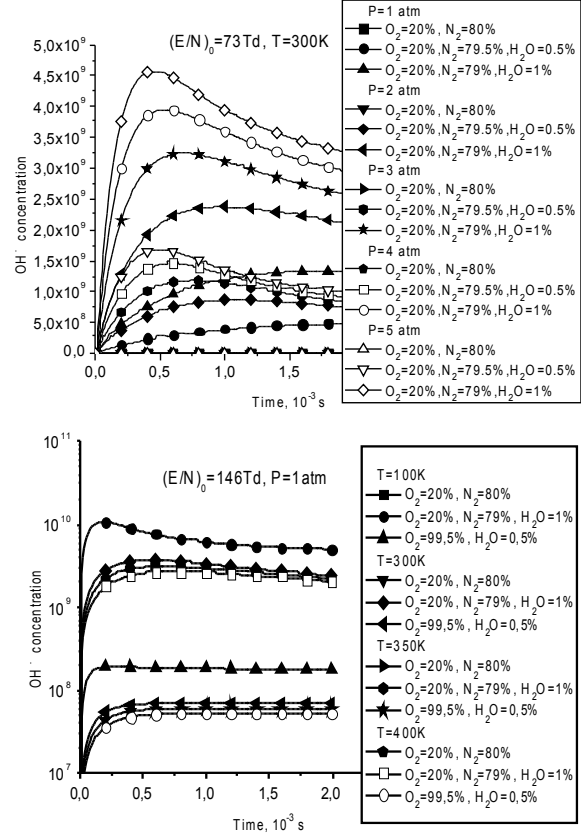


Fig. 7. Concentration of negative  $OH^-$  ions for various gas mixtures at different pressures and temperatures. The indicated marks for dry air can be neglected

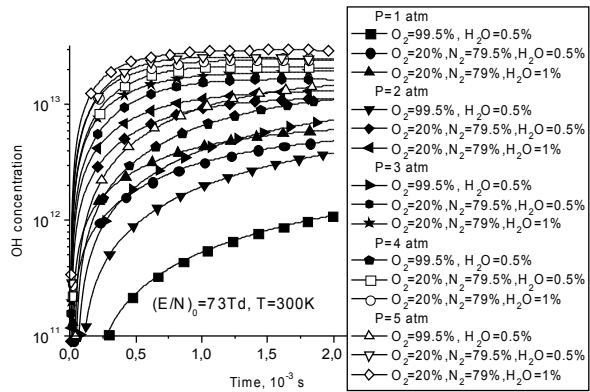


Fig. 8. Concentration of  $OH$  neutrals in various gas mixtures (humid) at different pressures

## Conclusion

Relying on the undertaken numerical simulation we have established that for humid air (with 1% water vapor content) with pressure rising from 1 atm. to 5 atm., the ozone concentration increases by a factor of 22 for a time of  $2 \times 10^{-3}$  s at a reduced electric field strength  $E/N \approx 73$  Td ( $1 \text{ Td} = 10^{-17} \text{ V/cm}^2$ ), i.e., an approximately square pressure dependence of the ozone concentration takes place, can be explained on the basis of the structure of basic reactions, where ozone is synthesized. In this case, the concentration of harmful  $NO_x$

compounds is 2 or 3 orders of magnitude lower than the ozone concentration; therefore, no excess of boundary-admissible concentrations of  $NO_x$  can be provided at rather high ozone concentrations.

For dry air, with a five-fold rise in pressure the electron concentration increases 35 times (from  $2 \cdot 10^6$  to  $7 \cdot 10^7 \text{ cm}^{-3}$ ). And at the same rise in pressure for the mixture  $O_2 : H_2O = 99,5 : 0,5$  the increase in the electron concentration does not exceed a factor of 6. As to the gas mixture  $N_2 : O_2 = 50 : 50$ , here the increase in the electron concentration does not exceed a factor of 3 at a five-fold rise in pressure.

The known fact of the rise in the discharge ignition voltage with an increasing ozone concentration was proposed to be treated relying on two facts: (i) the ion current is 20 to 40 times higher than the electron current, and (ii) as a result of a great cross section for attachment, the  $O_3^-$  ions are the basic ions, their concentration is more than 3 orders of magnitude higher than the concentration of electrons. Therefore, despite the fact that the ozone concentration makes about a few tenths of percent of the oxygen molecule concentration, and the both gases are electronegative, a high concentration of  $O_3^-$  ions (they are just responsible for the basic current transfer in the discharge) exerts a cardinal effect on

the current-voltage characteristic of the discharge, specifically, on the ignition voltage.

This work was supported in part by Science and Technology Center in Ukraine on project # 1069.

## References

1. R. Morrow // *Phys. Rev. A*. 1985, vol. 32, p.1799-1806.
2. Yu.S. Akishev, N.N. Elkin, A.P. Napartovich // *Plasma Physics Reports*. 1986, vol.12, p.1225-1234.
3. Yu.S. Akishev, I.V. Kochetov, A.I. Lobyko, A.P. Napartovich. // *Plasma Phys. Reports*. 2002, vol. 28, p.1054-1064.
4. V.I. Golota, V.I. Karas', V.P. Mal'khanov, I.F. Potapenko, O.N. Shulika. Proc. XXVIII Zvenigorod Conf. on Plasma Physics and CTF. Moscow, abstracts, 2001, p.161.
5. V.I. Golota, V.I. Karas', V.P. Mal'khanov, I.F. Potapenko, O.N. Shulika. Proc. XXIX Zvenigorod Conf. on Plasma Physics and CTF. Moscow, abstracts, 2002, p.164.
6. Ph.M. Morse, H. Feshbach. *Methods of Theoretical Physics*. New York, Toronto, London, McGraw-Hill Book Company, Inc. 1953. Part 2, p.886.

В результате теоретических исследований и численного моделирования представляем следующие выводы: для влажного воздуха при увеличении давления от  $1.0133 \cdot 10^5$  до  $5.0665 \cdot 10^5$  Па концентрация озона в течение  $2 \cdot 10^{-3}$  с становится выше в 22 раза. Этот факт мы объясняем структурой реакций, в которых производится озон. В этом случае концентрации вредных  $NO_x$  на 2-3 порядка ниже концентрации озона; (ii) показано, что азот полезен для производства озона в разряде; (iii) Основываясь на составе ионов мы объясняем увеличение напряжения зажигания разряда при возрастании концентрации озона даже при низкой концентрации озона сменой электронного тока ионным, причем основными являются отрицательные ионы  $O_3^-$ .

В результаті теоретичних досліджень та чисельного моделювання ми представляємо такі висновки: для вологого повітря при підвищенні тиску від  $1.0133 \cdot 10^5$  до  $5.0665 \cdot 10^5$  Па концентрація озону впродовж  $2 \cdot 10^{-3}$  с стає вищою в 22 рази. Цей факт ми пояснюємо структурою реакцій, в котрих отримується озон. В цьому випадку концентрації шкідливих  $NO_x$  на 2-3 порядки нижчі, ніж концентрація озону; (ii) показано, що азот корисний для генерації озону в розряді; (iii) На основі складу іонів ми пояснюємо збільшення напруги запалювання розряду при зростанні концентрації озону навіть при низькій концентрації озону заміною електронного струму іонним, причому основними є негативні іони  $O_3^-$ .